


RESEARCH PAPER



Inhibition of non-homologous end joining mitigates paclitaxel resistance resulting from mitotic slippage in non-small cell lung cancer

Kosuke Tsuji^a, Eiki Kikuchi ^{a,b}, Yuta Takashima^a, Tetsuaki Shoji^a, Hirofumi Takahashi^a, Shotaro Ito^a, Daisuke Morinaga^a, Masahiro Kashima^a, Makie Maeda^a, Hidenori Kitai^a, Junko Kikuchi^{a,b,c}, Jun Sakakibara-Konishi^a, and Satoshi Konno^a

^aDepartment of Respiratory Medicine, Faculty of Medicine, Hokkaido University, Sapporo, Japan; ^bKikuchi Medical–Respiratory Clinic, Sapporo, Japan; ^cDepartment of Clinical Cancer Genomics, Hokkaido University Hospital, Sapporo, Japan

ABSTRACT

Mitotic slippage, which enables cancer cells to bypass cell death by transitioning from mitosis to the G1 phase without undergoing normal cytokinesis, is one likely mechanism of paclitaxel (PTX) resistance. DNA double-strand breaks (DSBs) in the G1 phase are mainly repaired through non-homologous end joining (NHEJ). Therefore, inhibiting NHEJ could augment the PTX-induced cytotoxicity by impeding the repair of PTX-induced DSBs during the G1 phase following mitotic slippage. We aimed to evaluate the effects of NHEJ inhibition on mitotic slippage after PTX treatment in non-small cell lung cancer (NSCLC). H1299, A549, H1975, and H520 NSCLC cell lines were employed. In addition, A-196 and JQ1 were used as NHEJ inhibitors. H1299 cells were PTX-resistant and exhibited an increased frequency of mitotic slippage upon PTX treatment. NHEJ inhibitors significantly augmented the PTX-induced cytotoxicity, DSBs, and apoptosis in H1299 cells. The newly generated PTX-resistant cells were even more prone to mitotic slippage following PTX treatment and susceptible to the combined therapy. Docetaxel further demonstrated synergistic effects with the NHEJ inhibitor in PTX-resistant cells. NHEJ inhibition may overcome intrinsic or acquired PTX resistance resulting from mitotic slippage by synergistically increasing the cytotoxic effects of antimetabolic drugs in NSCLC.

ARTICLE HISTORY

Received 6 March 2023

Revised 8 July 2023

Accepted 30 July 2023

KEYWORDS

Mitotic slippage; non-homologous end joining; paclitaxel; non-small cell lung cancer; docetaxel; paclitaxel resistance


Introduction


Lung cancer is the leading cause of cancer-related mortality worldwide, with non-small cell lung cancer (NSCLC) accounting for approximately 85% of lung cancer cases [1–3]. Despite the efficacy of recently developed molecular-targeted drugs and immune checkpoint inhibitors, the survival rates of patients with advanced NSCLC remain poor [4,5]. Therefore, cytotoxic chemotherapeutic agents, including paclitaxel (PTX) and docetaxel (DTX), which are antimetabolic drugs that attenuate the depolymerization of microtubules, remain widely used for treatment.

PTX impairs microtubule dynamics by interrupting the proper attachment of microtubules to kinetochores, thereby activating the spindle assembly checkpoint (SAC), leading to mitotic arrest and DNA double-strand breaks (DSBs) [6]. However, in most cases, PTX resistance arises after several months of treatment [7].

Mitotic slippage, where cancer cells circumvent cell death by transitioning from the M to the G1 phase without normal cytokinesis, is one possible mechanism of PTX resistance [8]. After PTX induces cell arrest at the M phase, cells may either succumb to mitotic cell death or evade it by mitotic slippage. Therefore, those undergoing slippage either re-enter the cell cycle or die in the G1 phase.

Inhibition of DNA damage repair can augment the potency of DNA-damaging agents. In addition, non-homologous end joining (NHEJ) and homologous recombination (HR) are the primary mechanisms for repairing DSBs [9]. HR defects have been linked to increased sensitivity to platinum and poly (adenosine diphosphate ribose) polymerase (PARP) inhibitors in certain cancer types, such as breast cancer with BRCA mutation or prostate cancer with HR gene mutation. Consequently, these therapies have been widely implemented in clinical

CONTACT Eiki Kikuchi  eikik@med.hokudai.ac.jp  Department of Respiratory Medicine, Faculty of Medicine, Hokkaido University, N 15, W 7, Kita-ku 0608638, Japan

 Supplemental data for this article can be accessed online at <https://doi.org/10.1080/15384101.2023.2243761>

© 2023 Informa UK Limited, trading as Taylor & Francis Group

practice. However, the therapies targeting NHEJ have not been extensively investigated [10,11]. A-196, which is a potent and selective inhibitor of SUV420H1 and SUV420H2, reduces NHEJ-mediated DSB repair without affecting HR [12]. Moreover, JQ-1, which is a bromodomain and extra terminal domain inhibitor, suppresses gene expressions related to NHEJ and reduces NHEJ activity [13,14]. Because DSBs in G1 are exclusively repaired by NHEJ [9,15], NHEJ is likely the mechanism of DSB repair after mitotic slippage.

Therefore, we hypothesized that inhibiting NHEJ could augment PTX-induced cytotoxicity by impeding the repair of PTX-induced DSBs during G1 following mitotic slippage. Here, we aimed to evaluate the effects of NHEJ inhibition on mitotic slippage after PTX treatment in NSCLC cell lines.

Materials and methods

Reagents

PTX solution (10 mM) was purchased from Selleck Chemicals (Houston, TX, USA). A-196 (Cayman Chemical Company, Ann Arbor, MI, USA), JQ1 (Cayman Chemical Company), AZD7648 (Selleck Chemicals), and SCR7 (Selleck Chemicals) were dissolved in dimethyl sulfoxide (DMSO) to make stock solutions of 20, 20, 10, and 100 mM, respectively.

Cell culture

The four human NSCLC cell lines, including A549, H1299, H1975, and H520, were acquired from the American Type Culture Collection (Manassas, VA, USA) and maintained in RPMI-1640 medium supplemented with 10% fetal bovine serum (FBS) and 100 U/mL penicillin-streptomycin in a humidified atmosphere at 37°C with 5% CO₂. In addition, the human embryonic kidney cell line 293T was acquired from the Riken Bioresource Research Center (Tsukuba, Japan) and maintained in Dulbecco's Modified Eagle Medium supplemented with 10% heat-inactivated FBS under the same conditions. All cell lines were authenticated by the Japanese Collection of Research Bioresources Cell Bank (Osaka, Japan), using short tandem repeat profiling.

Cell proliferation assay

Antitumor activities of each drug applied singly and in combination were assessed using the MTT cell proliferation assay, according to the manufacturer's instructions (Promega Corporation, Madison, WI, USA). Cells were seeded in 96-well plates at a density of 2,000–6,000 cells per well and cultured for 24 h before drug treatment. After treatment for 72 h, cell viability was measured using Varioskan Flash (Thermo Fisher Scientific, Waltham, MA, USA). The half maximal inhibitory concentration (IC₅₀) was calculated using GraphPad Prism version 8.4.3 (GraphPad Software, San Diego, CA, USA).

Antibodies and Western blotting

Whole-cell lysates were subjected to Western blotting to analyze the expression of various proteins using the specific primary antibodies that followed at 4°C overnight. Anti-actin antibody (1:1500, #A2066) was purchased from Sigma-Aldrich (St. Louis, MO, USA). Furthermore, antibodies for cleaved PARP (1:1000, #5625), γ H2AX (Ser139) (1:1000, #2577), DNA-PKcs (1:1000, #38168), DNA ligase IV (1:1000, #14649), BRCA1 (1:1000, #14823), and Rad51 (1:1000, #8875) were purchased from Cell Signaling Technology (Danvers, MA, USA). ECL Anti-Rabbit IgG, Horseradish Peroxidase-Linked Whole Antibody (1:50000 for actin and 1:10000 for the others, NA934) (Global Life Sciences Solutions Operations UK Ltd, Little Chalfont, United Kingdom) was used as the secondary antibody for 24 h at room temperature. ECL Prime Western Blotting Detection Reagent (Global Life Sciences Solutions Operations UK Ltd) was used to detect chemiluminescent signals.

Cell cycle and apoptosis assays

Cell cycle and apoptosis assays were performed using a BD FACSVerse flow cytometer (Becton Dickinson, Franklin Lakes, NJ, USA). The cell cycle was analyzed using propidium iodide (PI)/RNase Staining Buffer (Becton Dickinson) and Alexa Fluor 647 Rat anti-Histone H3 (pS28) (Becton Dickinson), as per the manufacturer's

instructions. In addition, apoptosis was analyzed using Annexin V and PI with the MEBCYTO Apoptosis Kit (Annexin V-FITC kit) (MBL, Nagoya, Japan) and terminal deoxynucleotidyl transferase-mediated nick end labeling (TUNEL) assay with the MEBSTAIN Apoptosis TUNEL Kit Direct (MBL), as per the manufacturer's instructions. Annexin V positive-PI negative and Annexin V positive-PI positive populations indicated cells in early and late apoptosis, respectively. TUNEL positive populations indicated cells undergoing apoptosis.

In vitro NHEJ DNA repair assay

NHEJ reporter assay was performed using the chromosomally integrated green fluorescent protein (GFP) reporter pimeJ5GFP in H1299 (H1299-EJ5) and 293T cells (293T-EJ5), as previously reported [16,17]; pimeJ5GFP was a gift from Prof. Jeremy Stark (#44026; Addgene, Cambridge, MA, USA). The H1299-EJ5 and 293T-EJ5 cells expressed GFP after successful NHEJ repair of DSBs induced by I-SceI endonuclease. Here, because DsRed was transfected with I-SceI endonuclease using IsceI-GR-RFP plasmid (#17654; Addgene), the ratio of GFP-positive cells to DsRed-positive cells after I-SceI transfection directly correlated with NHEJ DNA repair activity. At 48 h after I-SceI transfection, GFP and DsRed expressions were analyzed using a flow cytometer. H1299-EJ5 and 293T-EJ5 cells were treated with 10 μ M A-196 or 0.2 μ M JQ1.

Live-cell imaging and microscopy

Cells were seeded in 35 mm dishes at a density of $4\text{--}10 \times 10^4$ cells and cultured for 24 h before cell cycle synchronization, which was conducted using a single 2 mM thymidine (Sigma-Aldrich) arrest. At 24 h after arrest, cells were released into media containing the following agents and analyzed: 100 nM PTX, 5 μ M A-196, 2 μ M JQ1, or the combination of these. DMSO was used as a solvent control. In addition, images were captured every 5 min for 24 h using a Bioevo BZ-9000 (Keyence, Osaka, Japan) with incubation at 37°C with 5% CO₂. The fates of at least 100 cells were tracked through the entire imaging period. Mitotic entry was

characterized by cell rounding and cell death by cell retraction, blebbing of the plasma membrane, and cessation of movement. Cell death was classified as death in mitosis when mitotic cells died before cell division or post-mitotic death (PMD) when the death occurred following mitotic slippage. Mitotic slippage was defined by mitotic exit without cell division.

Immunofluorescence staining

Analysis of mitotic catastrophes was conducted as previously reported [13,18–20]. For immunofluorescence staining, cells were treated with vehicle, 100 nM PTX, 5 μ M A-196, or the combination of these for 24 h. Cells were fixed using 4% paraformaldehyde for 20 min at 4°C and permeabilized with PBS containing 0.5% Triton X-100 for 10 min at 4°C. Subsequently, cells were incubated with Blocking One Histo (Nacalai Tesque, Kyoto, Japan) for 10 min at room temperature to block nonspecific antibody-binding sites. Next, cells were incubated with primary rabbit antibody for β -tubulin (1:100, #2128) (Cell Signaling Technology) and mouse antibody for pHH3 (1:400, #9706) (Cell Signaling Technology) at 4°C overnight. Then, they were incubated with Alexa Flour 488 Goat anti-Rabbit IgG (1:500, A11034) (Thermo Fisher Scientific) and Alexa Flour 594 Goat anti-Mouse IgG (1:500, A11032) (Thermo Fisher Scientific) for 90 min, followed by DAPI staining. Coverslips were mounted with a ProLong Diamond Antifade Mountant reagent (Thermo Fisher Scientific). Fluorescent microscopic analysis was performed using a Bioevo BZ-9000 (Keyence). At least 100 cells were counted from random microscopic fields for each condition in three independent experiments.

Small interfering RNA (siRNA)

DNA-PKcs, DNA ligase IV, BRCA1, and Rad51 RNA interference were performed using ON-TARGET plus siRNA SMART pool and ON-TARGET plus Nontargeting Control pool (Horizon Discovery, Cambridge, United Kingdom). Knockdown efficacy was assessed using Western blotting 24 h after transfection. For the cell proliferation assay, cells were seeded

and cultured for 24 h before transfection. After 24 h of transfection, PTX was added to the medium. After a 72 h treatment, cell viability was measured.

Statistical analysis

All data were derived from at least three independent experiments and are shown as means \pm standard deviation unless otherwise indicated. Differences between two or four groups were statistically analyzed using Welch's *t*-test or Dunnett's multiple comparisons test, respectively. Statistical significance was set at $p < 0.05$. Statistical analyses were performed using GraphPad Prism version 8.4.3 (GraphPad Software, San Diego, CA, USA).

Results

H1299 was PTX-resistant and showed a more frequent mitotic slippage after PTX treatment

We evaluated the antiproliferative effects of PTX on four NSCLC cell lines using an MTT cell proliferation assay. The results revealed that H1299 was resistant to PTX compared with the other cell lines (Supplementary Figure S1A and Table S1). Subsequently, we assessed the effect of PTX on the cell cycle and observed that all cell lines underwent mitotic arrest. Nevertheless, fewer mitotic cells were observed in H1299 than in the other cell lines (Figure 1a-b). Next, we measured the time elapsed from mitotic entry to anaphase after PTX treatment using time-lapse microscopy. We observed that, in H1299 cells, the mean duration of the normal cell division process was 100 min, significantly shorter than that observed in the other cell lines, suggesting a reduced effect of PTX on mitotic arrest (Supplementary Figure S1B and Table S2). We further counted the cells undergoing mitotic slippage using time-lapse microscopy and discovered that H1299 exhibited significantly more frequent mitotic slippage after PTX treatment (Figure 1c and Table 1). Overall, H1299 resisted PTX and showed a more frequent mitotic slippage after PTX treatment.

NHEJ inhibitors significantly enhanced the PTX-induced cytotoxicity, DSBs, and apoptosis in H1299

First, we assessed the effect of NHEJ inhibitors to explore the combined effect of NHEJ inhibitors and PTX. A-196 and JQ1 were found to suppress NHEJ efficacy (Supplementary Figure S2A–B). An MTT cell proliferation assay was utilized to evaluate the combined effects of NHEJ inhibitors and PTX, which revealed that A-196 or JQ1 significantly augmented the cytotoxic potency of PTX only in H1299 (Table 2; Supplementary Figure S2C–D and Table S3). Moreover, flow cytometry using annexin V and PI confirmed the synergistic effects of PTX and A-196 or JQ1 and revealed that the combination induced apoptosis (Figure 2a-b). Western blotting demonstrated that the combined therapy increased cleaved PARP and γ H2AX (Figure 2c-d). TUNEL assay confirmed that the combined therapy induced DSBs (Supplementary Figure 2E–F). Collectively, NHEJ inhibitors significantly enhanced the PTX-induced cytotoxicity, DSBs, and apoptosis.

To further validate the effect of NHEJ inhibition, we used additional NHEJ inhibitors, namely, the DNA-PKcs inhibitor AZD7648 and the DNA ligase IV inhibitor SCR7 [21,22]. Combined with these NHEJ inhibitors, the MTT cell proliferation assay demonstrated that PTX-induced cytotoxicity was augmented in H1299 (Supplementary Figure S3A–B and Table S4–6). Flow cytometry, Western blotting, and TUNEL assay revealed that the combination therapy induced apoptosis and DSBs in H1299 (Supplementary Figure S3C–H).

Next, we conducted knockdown experiments using siRNAs against DNA-PKcs (siDNA-PKcs) or DNA ligase IV (siDNA ligase IV) (Supplementary Figure S4A). The knockdown of either DNA-PKcs or DNA ligase IV significantly augmented the PTX-induced cytotoxicity compared to the control siRNA (Supplementary Figure S4B–C and Tables S7–8). Furthermore, we performed knockdown experiments using siRNAs against BRCA1 (siBRCA1) or Rad51 (siRad51) (Supplementary Figure S4D), which are essential components of the HR pathway [9]. The results demonstrated that siBRCA1 or siRad51 did not augment the PTX-induced cytotoxicity, indicating that NHEJ inhibition, rather than HR inhibition, significantly enhances PTX-induced cytotoxicity.

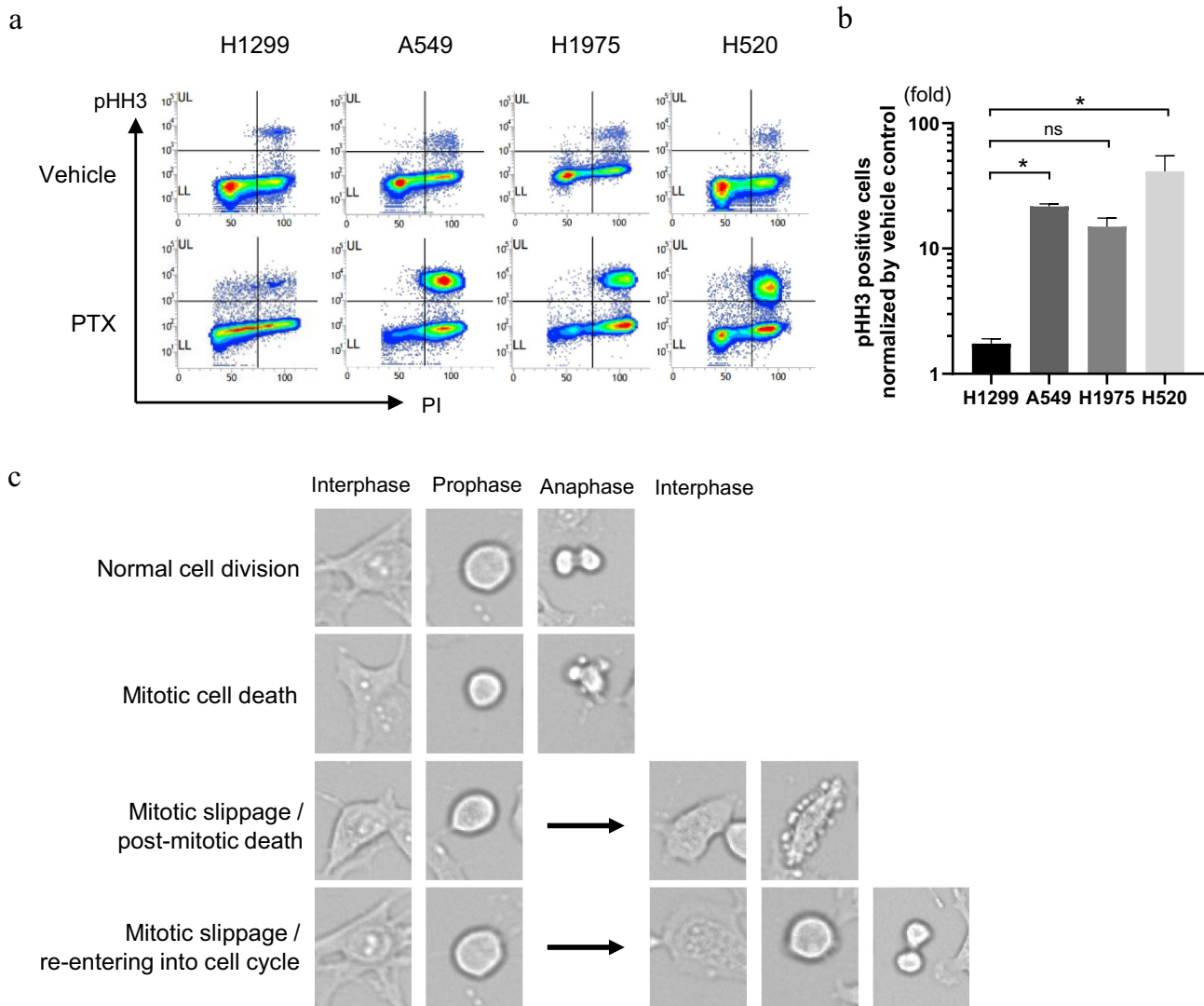


Figure 1. H1299 was PTX resistant and showed a more frequent mitotic slippage after PTX treatment. (a) Mitotic cells were analyzed using flow cytometry and pHh3/propidium iodide (PI) staining. Representative images of flow cytometry are shown. (b) Bar graphs showing summary data for flow cytometry normalized by vehicle control. Bars and error bars represent mean and SD, respectively ($n = 3/\text{group}$). $*p < 0.05$, $ns\ p \geq 0.05$, Dunnett's multiple comparisons tests. (c) Representative images of normal cell division, mitotic cell death, mitotic slippage and post-mitotic death, or mitotic slippage and reentering into the cell cycle. LL, lower left; LR, lower right; PTX, paclitaxel; UL, upper left; UR, upper right; SD, standard deviation.

Table 1. The number of cells undergoing mitotic slippage.

Cell line	Treatment	Slippage/Total cells	p-value
H1299	Vehicle	2/140	.01
	PTX	10/124	
A549	Vehicle	0/113	>.99
	PTX	0/158	
H1975	Vehicle	2/179	.68
	PTX	3/176	
H520	Vehicle	1/252	>.99
	PTX	1/265	
A549-PR	Vehicle	0/158	.03
	PTX	6/170	

Data represent the mean \pm SD of three independent experiments. PTX, paclitaxel; SD, standard deviation.

Table 2. IC₅₀ of paclitaxel ±2.5 μM of A-196.

Cell line	PTX	PTX + A-196	p-value
H1299	37.4 ± 2.9	18.2 ± 1.7	<.01
A549	8.1 ± .8	6.8 ± 1.3	.31
H1975	3.6 ± 1.0	3.9 ± .6	.69
H520	8.9 ± .9	8.1 ± .8	.39
A549-PR	63.8 ± 7.0	3.8 ± 1.5	.02

Data represent the mean ± SD of three independent experiments. PTX, paclitaxel; SD, standard deviation.

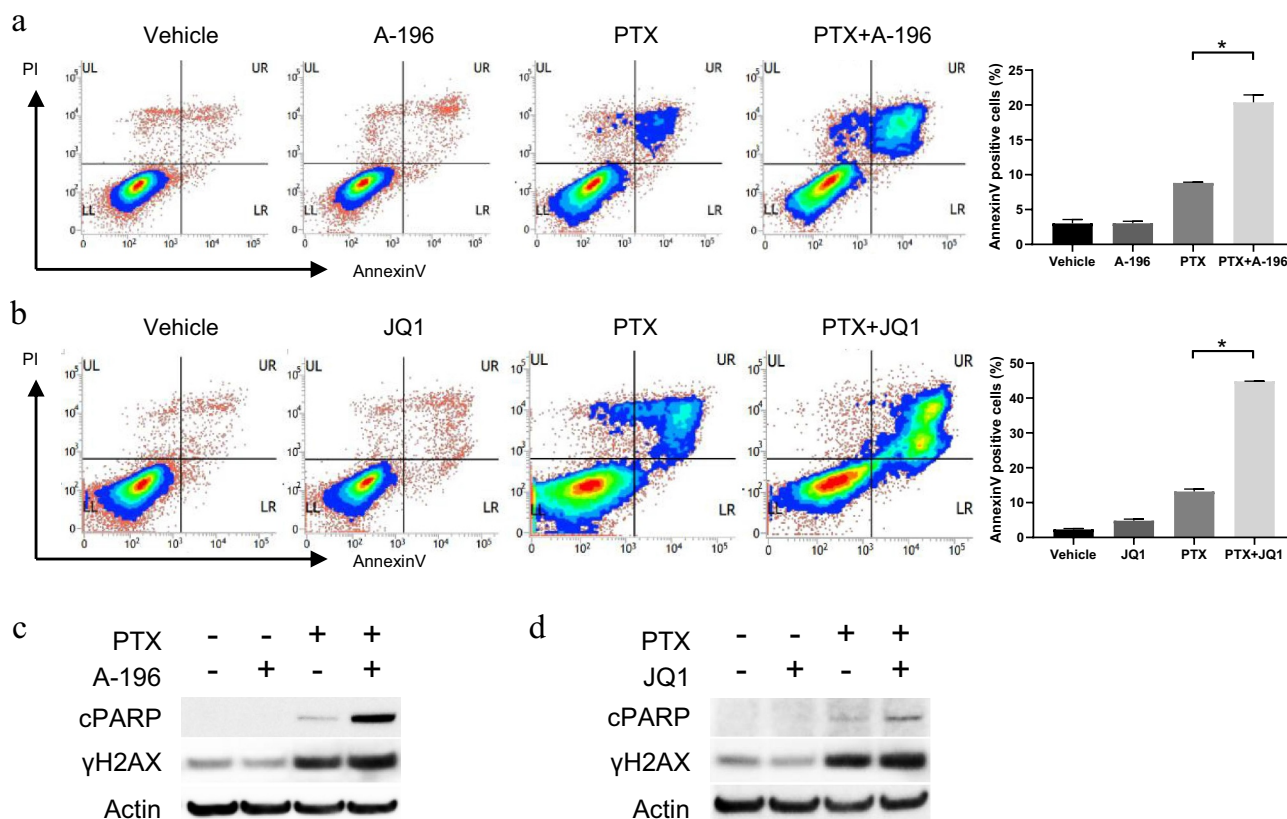


Figure 2. NHEJ inhibitors significantly enhanced the PTX-induced cytotoxicity, DSB, and apoptosis in H1299. (A – B) Flow cytometry showing apoptotic cells by Annexin V/propidium iodide (PI) staining after treatment with PTX and A-196 (a) or PTX and JQ1 (b). Representative images of flow cytometry are shown. Bar graphs show summary data of flow cytometry. Bars and error bars represent mean and SD, respectively ($n = 3/\text{group}$). * $p < 0.05$, Welch t -test. (C – D) Western blotting of cleaved PARP and γ H2AX in cells treated with PTX and A-196 (c) or PTX and JQ1 (d). DSB, double-strand break; LL, lower left; LR, lower right; NHEJ, non-homologous end joining; PARP, poly (adenosine diphosphate-ribose) polymerase; PTX, paclitaxel; UL, upper left; UR, upper right.

NHEJ inhibitors augmented cell death following mitotic slippage without affecting aberrant mitosis

We speculated that the NHEJ inhibitor could augment PTX-induced cell death by hindering the repair of PTX-induced DSBs during the G1 phase following mitotic slippage. Therefore, we investigated PMD after the mitotic slippage using time-lapse microscopy. After the combined treatment of PTX and A-196 or JQ1, PMD increased in H1299 (Supplementary Table

S10). Moreover, the elapsed time from mitotic slippage to PMD after the combined treatments was significantly reduced to less than half that observed after PTX monotherapy (Figure 3a).

Therefore, we conducted immunofluorescence staining to observe the mitotic alterations to further elucidate the effects of the combination of PTX and A-196 on mitosis. We confirmed that rounding cells observed in optical microscopy images were positive for pHH3 and defined cell

rounding as a characteristic of mitotic entry in time-lapse microscopy, consistent with previous reports [8,23] (Figure 1c and 3b). Abnormal mitosis, including misaligned chromosomes, dispersed chromosomes, and disorganized multipolar spindles, were observed in H1299 after treatment with either PTX monotherapy or the combined therapy of PTX and A-196 (Figure 3b). Quantification of

cells with aberrant nuclei, such as micronuclei, multi-lobular nuclei, and fragmented nuclei, revealed that PTX markedly increased the cells with aberrant nuclei. However, adding the NHEJ inhibitor did not enhance the mitotic catastrophe (Figure 3c-d). These findings indicate that NHEJ inhibitors augment cell death following mitotic slippage without affecting aberrant mitosis.

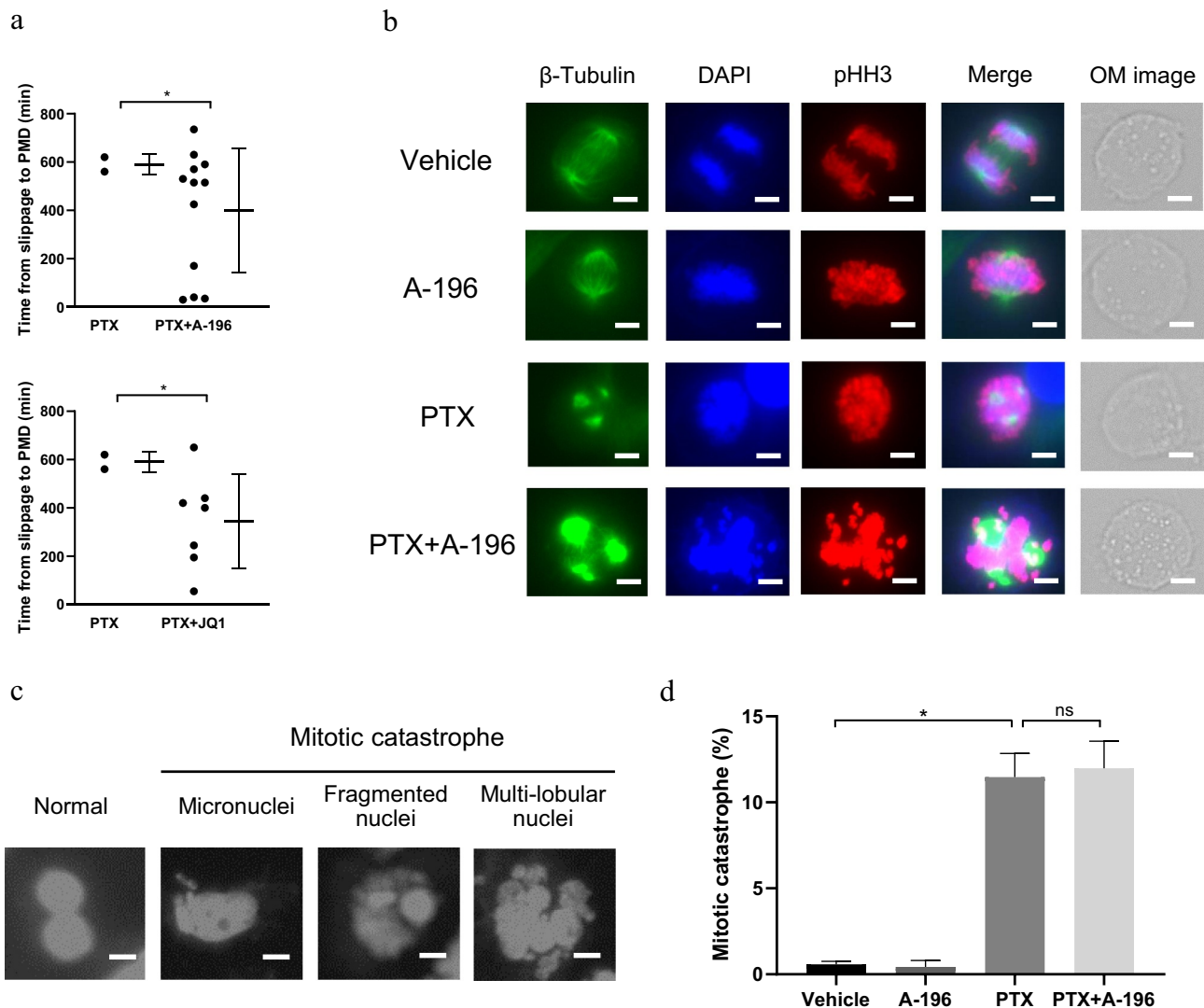


Figure 3. Post-mitotic death and mitotic catastrophe were induced by the combination of PTX and NHEJ inhibitors in H1299. (a) The elapsed time from mitotic slippage to post-mitotic death. The fates of at least 100 cells were tracked throughout the entire imaging period for each condition in three independent experiments. Each spot represents one H1299 cell undergoing PMD. $*p < 0.05$, Welch *t*-test. (b) Representative images of abnormal mitoses in H1299 after treatment with PTX, A-196, or the combination. Scale bars represent 10 μ m. (c) Representative images of H1299 possess features of mitotic catastrophes, such as micronuclei, fragmented nuclei, and multi-lobular nuclei. Scale bars represent 10 μ m. (d) Bar graphs show percentages of cells that exhibited features of mitotic catastrophe in H1299 after treatment with PTX, A-196, or the combination. Bars and error bars represent mean and SD ($n = 3$). ns, $p \geq 0.05$, Welch *t*-test. DAPI, 4',6-diamidino-2-phenylindole; NHEJ, non-homologous end joining; OM, optimal microscopy; PARP, poly (adenosine diphosphate-ribose) polymerase; PMD, post-mitotic death; PTX, paclitaxel.

Newly generated PTX-resistant cells showed a more frequent mitotic slippage after PTX treatment and were more susceptible to the combined therapy

We investigated the consequences of NHEJ inhibition on PTX resistance by utilizing newly generated PTX-resistant cells. Therefore, we developed the PTX-resistant lung cancer cells, A549-PR, which were established by exposing A549 cells to gradually increasing concentrations of PTX. Subsequently, we quantified the cells undergoing mitotic slippage and evaluated the combined effects of NHEJ inhibitors and PTX. The results indicated that A549-PR exhibited more frequent mitotic slippage after PTX treatment than the parent A549 (Table 1). Furthermore, administering A-196 significantly augmented the PTX-induced cytotoxicity (Table 2; Supplementary Figure S5A). Flow cytometry, Western blotting, and TUNEL assay additionally revealed that the combination therapy elicited apoptosis and DSBs (Figure 4a-b; Supplementary Figure S5B-C).

DTX showed the combined effects with the NHEJ inhibitor in PTX-resistant cells

To expand these findings to clinical application, we explored the potential of combining NHEJ inhibitors with an analogous antimetabolic agent, DTX, a standard chemotherapeutic agent for the previously treated NSCLC [24]. MTT cell proliferation assay demonstrated that PTX-resistant cells were also DTX-resistant and that A-196 significantly augmented the DTX-induced cytotoxicity in A549-PR rather than in parent A549 (Supplementary Figure S6A-B and Tables S1, S11). Flow cytometry using annexin V and PI confirmed the combination-induced apoptosis (Figure 4c; Supplementary Figure S6C). In addition, Western blotting revealed that the combined therapy increased cleaved PARP and γ H2AX (Figure 4d). TUNEL assay further confirmed DSBs in combined therapy (Supplementary Figure 6D). Therefore, our results suggested that a concomitant regimen of an NHEJ inhibitor can significantly augment the DTX-induced cytotoxicity, DSBs, and apoptosis.

Discussion

We demonstrated that mitotic slippage occurred more frequently in both intrinsic and acquired PTX-resistant cell lines and that the inhibition of NHEJ could augment PTX-induced cytotoxicity by impeding the repair of PTX-induced DSBs following mitotic slippage (Figure 4e). We ascertained that H1299 cells were innately PTX-resistant, whereas A549-PR cells were acquired PTX-resistant. These cell lines demonstrate a decreased effect of PTX on mitotic arrest and a higher frequency of mitotic slippage. Therefore, we directly showed a correlation between mitotic slippage and PTX resistance using time-lapse microscopy.

Several reports have demonstrated attempts to suppress mitotic slippage using small molecular compounds or siRNAs that target various molecules involved in the cell division process [23,25]; however, clinical success has been elusive. We have proposed an approach to induce cell death after mitotic slippage by impeding DNA damage repair rather than inhibiting mitotic slippage. Furthermore, the choice between NHEJ and HR as a method of DNA damage repair depends primarily on the cell cycle stage [26]. NHEJ is active throughout the cell cycle phase except for the mitotic phase. In contrast, little repair of DNA damage occurs in the mitotic phase. Under normal conditions, DNA damage in the mitotic phase is detected and marked for repair after mitotic exit, mainly by NHEJ in the G1 phase [15], while the choice of DNA repair pathway after mitotic slippage remains poorly understood. The cells undergoing mitotic slippage are believed to enter the G1 phase with DNA damage [27]. Therefore, we focused on the importance of NHEJ in DNA repair after mitotic slippage.

A-196 is a chemical probe that potently and selectively inhibits SUV420H1 and SUV420H2, which facilitate proficient NHEJ-mediated DSB repair by catalyzing the di- and trimethylation of lysine 20 on histone H4 [12]. A-196 inhibits 53BP1 foci formation and reduces NHEJ-mediated DSB repair without affecting HR. JQ-1 is a bromodomain and extra terminal domain inhibitor that suppresses gene expressions related to NHEJ and reduces NHEJ activity [13,14]. In addition to these, several NHEJ inhibitors have been developed. DNA-PK inhibitors,

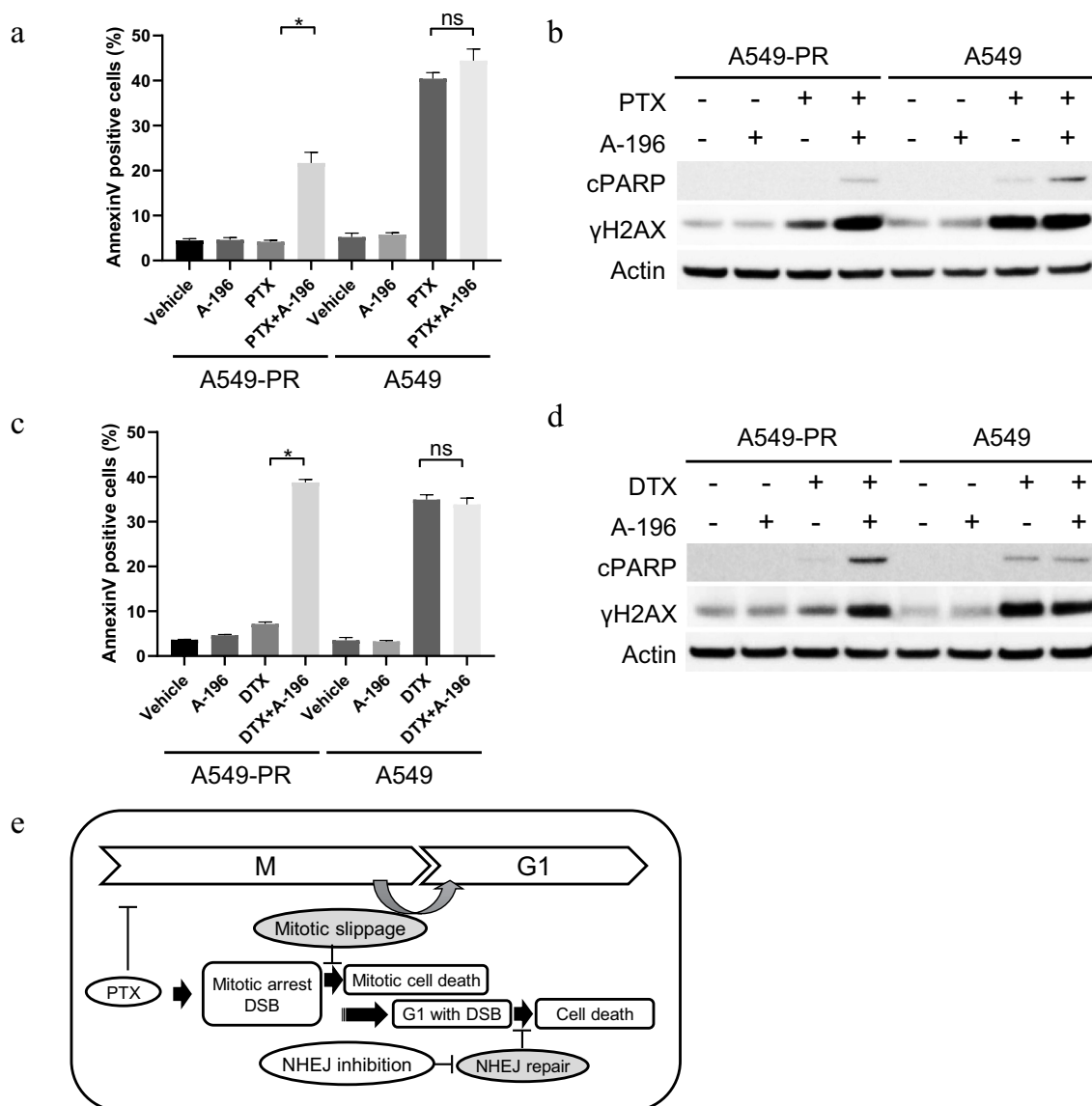


Figure 4. A newly generated PTX-resistant cell line showed a more frequent mitotic slippage after PTX treatment and was more susceptible to the combined therapy. (a and c) Apoptotic cells were analyzed using flow cytometry and Annexin V/propidium iodide (PI) staining after treatment with PTX and A-196 (A) or DTX and A-196 (c). Bar graphs show summary data for flow cytometry. Bars and error bars represent mean and SD, respectively ($n = 3/\text{group}$). * $p < 0.05$, $ns \geq 0.05$, Welch t -test. (b and d) Western blotting of cleaved PARP and γ H2AX in cells treated with PTX and A-196 (b) or DTX and A-196 (d). (e) Schematic of mitotic slippage and NHEJ inhibition. DTX, docetaxel; NHEJ, non-homologous end joining; PARP, poly (adenosine diphosphate-ribose) polymerase; PMD, post-mitotic death; PTX, paclitaxel; SD, standard deviation.

including M3814 and AZD7648, and DNA ligase IV inhibitors, such as SCR7, target NHEJ-mediated protein, resulting in NHEJ inhibition [21,22,28]. Because there are currently no clinically available inhibitors of NHEJ, the exploration of NHEJ inhibitors is crucial.

We have shown that combining PTX and NHEJ inhibitors could be advantageous in treating PTX resistance caused by mitotic slippage. Additionally,

we demonstrated the efficacy of an NHEJ inhibitor in concert with DTX, which is a taxane analog in the same class as PTX and a standard chemotherapeutic agent for the previously treated NSCLC [24]. Consequently, combining DTX and NHEJ inhibitors may be a viable strategy to overcome PTX resistance resulting from mitotic slippage.

Mitotic slippage has been reported to be affected by SAC [29]. SAC is a mitotic surveillance

mechanism that arrests mitotic progression during cell cycle dysfunction and ensures proper chromosome alignment before controlled segregation of the chromosomes [25]. Mitotic exit, including normal cell division and mitotic slippage, occurs when cyclin B1 is degraded by the anaphase-promoting complex/cyclosome and its targeting subunit CDC20. Although SAC activation results in prolonged mitotic arrest followed by mitotic cell death, SAC silencing results in normal cell division or mitotic slippage [30]. The SAC activity is mediated by the SAC proteins, such as MAD2 and p31^{comet} [31]. Therefore, we evaluated the difference between A549-PR and A549 using Western blotting and quantitative reverse transcription-PCR to assess the molecular mechanisms of mitotic slippage. However, the expression of proteins and mRNAs related to the cell cycle and SAC, such as CDK4, CDK6, MAD2, p31^{comet}, and cyclinB1, did not differ between these cell lines (data not shown). Other factors may need to be investigated to assess the mechanistic link between mitotic slippage and PTX resistance in the future.

In conclusion, NHEJ inhibition may overcome intrinsic or acquired PTX resistance resulting from mitotic slippage by synergistically augmenting the cytotoxic effects of antimetabolic drugs in NSCLC.

Disclosure statement

No potential conflict of interest was reported by the author(s).

Funding

This research was supported by JSPS KAKENHI Grant Number JP20K07607.

Author contributions

Kosuke Tsuji and Eiki Kikuchi: Conceptualization, formal analysis, and drafting of the manuscript. All authors: Collecting the data and approving the results and conclusions.

Data availability statement

The authors confirm that the data supporting the findings of this study are available within the article and its supplementary materials.

ORCID

Eiki Kikuchi  <http://orcid.org/0000-0003-4098-6321>

References

- [1] Siegel RL, Miller KD, Fuchs HE, et al. Cancer statistics, 2021. *CA Cancer J Clin.* 2021 Jan;71(1):7–33. doi: [10.3322/caac.21654](https://doi.org/10.3322/caac.21654)
- [2] Sung H, Ferlay J, Siegel RL, et al. Global cancer statistics 2020: GLOBOCAN estimates of incidence and mortality worldwide for 36 cancers in 185 countries. *CA A Cancer J Clin.* 2021 May;71(3):209–249. doi: [10.3322/caac.21660](https://doi.org/10.3322/caac.21660)
- [3] Herbst RS, Heymach JV, Lippman SM. Lung cancer. *N Engl J Med.* 2008 Sep;359(13):1367–1380. doi: [10.1056/NEJMra0802714](https://doi.org/10.1056/NEJMra0802714)
- [4] Hirsch FR, Scagliotti GV, Mulshine JL, et al. Lung cancer: current therapies and new targeted treatments. *Lancet.* 2017;389(10066):299–311. doi: [10.1016/s0140-6736\(16\)30958-8](https://doi.org/10.1016/s0140-6736(16)30958-8)
- [5] Reck M, Remon J, Hellmann MD. First-line immunotherapy for non-small-cell lung cancer. *J Clin Oncol.* 2022 Feb, 20;40(6):586–597. doi: [10.1200/JCO.21.01497](https://doi.org/10.1200/JCO.21.01497)
- [6] Lara-Gonzalez P, Westhorpe FG, Taylor SS. The spindle assembly checkpoint. *Curr Biol.* 2012 Nov, 20;22(22):R966–R980. doi: [10.1016/j.cub.2012.10.006](https://doi.org/10.1016/j.cub.2012.10.006)
- [7] Sandler A, Gray R, Perry MC, et al. Paclitaxel-carboplatin alone or with bevacizumab for non-small-cell lung cancer. *N Engl J Med.* 2006 Dec;355(24):2542–2550. doi: [10.1056/NEJMoa061884](https://doi.org/10.1056/NEJMoa061884)
- [8] Hino M, Iemura K, Ikeda M, et al. Chromosome alignment-maintaining phosphoprotein CHAMP1 plays a role in cell survival through regulating Mcl-1 expression. *Cancer Sci.* 2021 Sep;112(9):3711–3721. doi: [10.1111/cas.15018](https://doi.org/10.1111/cas.15018)
- [9] Brandsma I, Gent DC. Pathway choice in DNA double strand break repair: observations of a balancing act. *Genome Integr.* Nov 27 2012;3(1):9. doi: [10.1186/2041-9414-3-9](https://doi.org/10.1186/2041-9414-3-9)
- [10] Robson M, Im SA, Senkus E, et al. Olaparib for metastatic breast cancer in patients with a germline BRCA mutation. *N Engl J Med.* 2017 Aug, 10;377(6):523–533. doi: [10.1056/NEJMoa1706450](https://doi.org/10.1056/NEJMoa1706450)
- [11] de Bono J, Mateo J, Fizazi K, et al. Olaparib for metastatic castration-resistant prostate cancer. *N Engl J Med.* 2020 May, 28;382(22):2091–2102. doi: [10.1056/NEJMoa1911440](https://doi.org/10.1056/NEJMoa1911440)
- [12] Bromberg KD, Mitchell TR, Upadhyay AK, et al. The SUV4-20 inhibitor A-196 verifies a role for epigenetics in genomic integrity. *Nat Chem Biol.* 2017 Mar;13(3):317–324. doi: [10.1038/nchembio.2282](https://doi.org/10.1038/nchembio.2282)
- [13] Takashima Y, Kikuchi E, Kikuchi J, et al. Bromodomain and extraterminal domain inhibition

- synergizes with WEE1-inhibitor AZD1775 effect by impairing non-homologous end joining and enhancing DNA damage in non-small cell lung cancer. *Int J Cancer*. 2020 Feb; 15;146(4):1114–1124. doi: [10.1002/ijc.32515](https://doi.org/10.1002/ijc.32515)
- [14] Stanlie A, Yousif AS, Akiyama H, et al. Chromatin reader Brd4 functions in Ig class switching as a repair complex adaptor of non-homologous end-joining. *Mol Cell*. 2014 Jul 3;55(1):97–110. doi: [10.1016/j.molcel.2014.05.018](https://doi.org/10.1016/j.molcel.2014.05.018)
- [15] Heijink AM, Krajewska M, van Vugt MA. The DNA damage response during mitosis. *Mutat Res*. 2013 Oct;750(1–2):45–55. doi: [10.1016/j.mrfmmm.2013.07.003](https://doi.org/10.1016/j.mrfmmm.2013.07.003)
- [16] Bennardo N, Cheng A, Huang N, et al. Alternative-NHEJ is a mechanistically distinct pathway of mammalian chromosome break repair. *PLoS Genet*. 2008 Jun, 27;4(6):e1000110. doi: [10.1371/journal.pgen.1000110](https://doi.org/10.1371/journal.pgen.1000110)
- [17] Gupta R, Somyajit K, Narita T, et al. DNA repair network analysis reveals shieldin as a key regulator of NHEJ and PARP inhibitor sensitivity. *Cell*. 2018 May 3;173(4):972–988 e23. doi: [10.1016/j.cell.2018.03.050](https://doi.org/10.1016/j.cell.2018.03.050)
- [18] Suzuki M, Yamamori T, Yasui H, et al. Effect of MPS1 inhibition on genotoxic stress responses in murine tumour cells. *Anticancer Res*. 2016;36(6):2783–2792.
- [19] Suzuki M, Yamamori T, Bo T, et al. MK-8776, a novel Chk1 inhibitor, exhibits an improved radiosensitizing effect compared to UCN-01 by exacerbating radiation-induced aberrant mitosis. *Transl Oncol*. 2017 Aug;10(4):491–500. doi: [10.1016/j.tranon.2017.04.002](https://doi.org/10.1016/j.tranon.2017.04.002)
- [20] Shoji T, Kikuchi E, Kikuchi J, et al. Evaluating the immunoproteasome as a potential therapeutic target in cisplatin-resistant small cell and non-small cell lung cancer. *Cancer Chemother Pharmacol*. 2020 May;85(5):843–853. doi: [10.1007/s00280-020-04061-9](https://doi.org/10.1007/s00280-020-04061-9)
- [21] Fok JHL, Ramos-Montoya A, Vazquez-Chantada M, et al. AZD7648 is a potent and selective DNA-PK inhibitor that enhances radiation, chemotherapy and olaparib activity. *Nat Commun*. 2019 Nov 7;10(1):5065. doi: [10.1038/s41467-019-12836-9](https://doi.org/10.1038/s41467-019-12836-9)
- [22] Srivastava M, Nambiar M, Sharma S, et al. An inhibitor of non-homologous end-joining abrogates double-strand break repair and impedes cancer progression. *Cell*. 2012 Dec, 21;151(7):1474–1487. doi: [10.1016/j.cell.2012.11.054](https://doi.org/10.1016/j.cell.2012.11.054)
- [23] Pena-Blanco A, Haschka MD, Jenner A, et al. Drp1 modulates mitochondrial stress responses to mitotic arrest. *Cell Death Differ*. 2020 Sep;27(9):2620–2634. doi: [10.1038/s41418-020-0527-y](https://doi.org/10.1038/s41418-020-0527-y)
- [24] Garon EB, Ciuleanu TE, Arrieta O, et al. Ramucirumab plus docetaxel versus placebo plus docetaxel for second-line treatment of stage IV non-small-cell lung cancer after disease progression on platinum-based therapy (REVEL): a multicentre, double-blind, randomised phase 3 trial. *Lancet*. 2014 Aug 23;384(9944):665–673. doi: [10.1016/S0140-6736\(14\)60845-X](https://doi.org/10.1016/S0140-6736(14)60845-X)
- [25] Henriques AC, Silva PMA, Sarmiento B, et al. Antagonizing the spindle assembly checkpoint silencing enhances paclitaxel and Navitoclax-mediated apoptosis with distinct mechanistic. *Sci Rep*. 2021 Feb 18;11(1):4139. doi: [10.1038/s41598-021-83743-7](https://doi.org/10.1038/s41598-021-83743-7)
- [26] van Gent, DC, Kanaar R, van Gent DC. Exploiting DNA repair defects for novel cancer therapies. *Mol Biol Cell*. 2016 Jul15;27(14):2145–2148. doi: [10.1091/mbc.E15-10-0698](https://doi.org/10.1091/mbc.E15-10-0698)
- [27] Hyun SY, Rosen EM, Jang YJ. Novel DNA damage checkpoint in mitosis: mitotic DNA damage induces re-replication without cell division in various cancer cells. *Biochem Biophys Res Commun*. 2012 Jul 6;423(3):593–599. doi: [10.1016/j.bbrc.2012.06.023](https://doi.org/10.1016/j.bbrc.2012.06.023)
- [28] van Bussel, MTJ, Awada A, de Jonge, MJA, et al. A first-in-man phase 1 study of the DNA-dependent protein kinase inhibitor peposertib (formerly M3814) in patients with advanced solid tumours. *Br J Cancer*. 2021 Feb;124(4):728–735. doi: [10.1038/s41416-020-01151-6](https://doi.org/10.1038/s41416-020-01151-6)
- [29] Sinha D, Duijf PHG, Khanna KK. Mitotic slippage: an old tale with a new twist. *Cell Cycle*. 2019 Jan;18(1):7–15. doi: [10.1080/15384101.2018.1559557](https://doi.org/10.1080/15384101.2018.1559557)
- [30] Zeng X, Xu WK, Lok TM, et al. Imbalance of the spindle-assembly checkpoint promotes spindle poison-mediated cytotoxicity with distinct kinetics. *Cell Death Dis*. 2019;10(4):314. doi: [10.1038/s41419-019-1539-8](https://doi.org/10.1038/s41419-019-1539-8)
- [31] Lok TM, Wang Y, Xu WK, et al. Mitotic slippage is determined by p31(comet) and the weakening of the spindle-assembly checkpoint. *Oncogene*. 2020;39(13):2819–2834. doi: [10.1038/s41388-020-1187-6](https://doi.org/10.1038/s41388-020-1187-6)